Magnetic Bearings for a High-Performance Optical Disk Buffer*

Richard Hockney and Timothy Hawkey

SatCon Technology Corporation
71 Rogers Street
Cambridge, Massachusetts

S/5-37
/63495
P- 14

ABSTRACT

An optical disk buffer concept can provide gigabit-per-second data rates and terabit capacity through the use of arrays of solid state lasers applied to a stack of erasable/reusable optical disks. The RCA optical disk buffer has evoked interest by NASA for space applications. The porous graphite air bearings in the rotary spindle as well as those used in the linear translation of the read/write head would be replaced by magnetic bearings or mechanical (ball or roller) bearings. Based upon past experience, roller or ball bearings for the translation stages are not feasible. Unsatisfactory, although limited experience exists with ball bearing spindles also. Magnetic bearings, however, appear ideally suited for both applications.

The use of magnetic bearings is advantageous in the optical disk buffer because of the absence of physical contact between the rotating and stationary members. This frictionless operation leads to extended life and reduced drag. The manufacturing tolerances that are required to fabricate magnetic bearings would also be relaxed from those required for precision ball and gas bearings. Since magnetic bearings require no lubricant, they are inherently compatible with a space (vacuum) environment. Magnetic bearings also allow the dynamics of the rotor/bearing system to be altered through the use of active control. This provides the potential for reduced vibration, extended regions of stable operation, and more precise control of position.

INTRODUCTION

The advent of optical disk recording technology has made possible a family of high data rate, high capability memory devices. These devices provide gigabit-per-second data rates and terabit capability through the use of arrays of solid state lasers applied to an optical disk stack. Bearings are an enabling technology area where improvements are required to allow these systems to be utilized in space applications. Air bearings, utilized in ground based systems, are impractical in space. Experience with rolling element bearings has been unsatisfactory. With proper development, magnetic bearings represent an ideal candidate for both the translational and rotation stages of these devices.

The purpose of this study was to define specifications and determine candidate magnetic hardware, sensor, and electronics specifications for the translator magnetic bearings to be retrofit into the optical disk buffer system. The work consisted of the determination of detailed performance requirements, the analyses of the capabilities of various bearing configurations, the selection of a baseline hardware and sensor configuration, and the determination of controller and electronics requirements. Successful completion of these tasks is considered evidence of the technical feasibility of applying magnetic bearing technology to this device.

It was found that the retrofit of magnetic bearings into the current system is very feasible with only minor modifications to the current system. A permanent-magnet biased, asymmetrical three-pole design was chosen for the translator bearing. The required electromagnetic hardware fits easily inside the available volume and has reasonable power consumption. The capacitive position sensors are small and have excellent resolution and linearity. The controller requirements are modest as are the remaining analog electronic functions which need to be implemented. The extension of this design definition to the detailed design required for prototype development would appear to be an extremely straightforward effort.

SPECIFICATIONS

Definition of the specifications for the magnetic bearings for the optical disk buffer was facilitated by the decision to make the baseline design capable of retrofit into the existing NASA/RCA buffer design. This then determined both the maximum dimensions and allowed volume for the electromagnetic hardware and the amount of suspended mass. The stiffness required was determined from a calculation of the static stiffness of the existing air bearings.

The structural modes of the supported structures were established by RCA using finite-element model analysis of the existing devices. Since the linear motor on the translator head would be replicated, its velocity and acceleration profiles were required. Finally, the maximum level of stray magnetic fields both in the area of the recording head and near the disk were established from knowledge of the sensitivity of the magnetic domains in the recording material. The detailed specifications for the translator magnetic bearings are listed in Table 1.

MAGNETIC DESIGN

The prime objective of the translator bearing design was the definition of a magnetic-bearing alternative requiring minimal modifications of the existing system. The current system is shown in Figures 1 and 2. The read/write head is mounted in the aluminum carriage between the linear motors, which are the heart of the whole assembly. Producing high forces, the linear motors use large samarium-cobalt magnets that create large magnetic fields in the air-gap (1.2 Tesla). The shafts that carry the return flux are therefore large and double as air bearing surfaces. Actually, the air bearings

Table 1. Specifications

Stiffness		
Parallel to disk	4.6×10^5	N/m
Normal to disk	7.0×10^5	N/m
Suspended mass	0.45	kg
First-mode frequency	1967	Hz
Maximum dimensions		
Length	3.8	cm
Width	4.4	cm
Height	4.4	cm
Maximum stray field		
At read/write head	3	mT
At disk surface	0.2	T
Maximum acceleration	21	m/s^2
Maximum velocity	1.2	m/s

are made by milling slots in the iron shaft and covering them with porous graphite. Air is then pumped through the slots and graphite, forming a cushion of air between the graphite and the aluminum carriage which it supports.

For an easy retrofit, the entire bearing and shaft structure cannot occupy more space than the current air bearing shaft does. As such, the geometric constraints were the most restrictive. The tight spacing drove many of the design parameters and eliminated many configuration options. A second major restriction was imposed by magnetic flux of the linear motors. The twin voice-coil motors must move the read/write heads at high acceleration and, as such, require large magnetic flux density. This means that there must be a large pole face facing the linear motor magnet (for uniform flux), and that the shaft must have sufficient cross sectional area to carry the return flux of the motor magnet back to its other pole.

Together these restrictions quickly narrowed the design options to the two shown in Figures 3 and 4. Normally, a radially symmetrical four- or eight-pole design is used for magnetic bearings, but the linear motor magnet flux prevented pole placement on one side. Fortunately, all five controlled degrees of freedom can be controlled with a three-pole design because the two bearing sets are mirror images of each other and can be coupled to provide the proper support. The design shown in Figure 4 was chosen as the candidate configuration because its layout is both simpler mechanically and had lower predicted internal flux density (0.8 T as opposed to 1.8 T). In both cases, a permanent magnet providing bias flux has been included. The bias flux is used because it provides a linear operating point and because it reduces power consumption while increasing force capability.

The detailed mechanical design was determined mainly by force requirements. It was assumed that under worst case loading (one gravity), the transient force requirements for stabilization would not exceed twice the weight of the translator-plus-bearing assembly (6.4

N). The pole face area (A) and bias magnetic field (B_O) are related to the force required through

$$F = \frac{2B_O{}^2A}{\mu_O} \qquad (1)$$

The pole face area is constrained by available space, so B_O is determined at the modest value of 0.14 Tesla. The other major variable to be determined was the air gap length, the trade-off being between reduced coil size and ease of construction - a smaller gap length allowing smaller coils to be used, but also requiring better part tolerances and more difficulty of production. Air bearings often use gaps as small as 0.013 mm, and magnetic bearings usually use air gaps between 0.2 and 0.4 mm. A median value of 0.3 mm was chosen as a compromise, being small enough to allow reasonable size coils, but large enough not to present great difficulties in manufacturing.

The magnetic design began with the permanent magnet which provides bias flux in the air gaps. The flux travels through three separate paths with two air gaps on each path. Since the translator is very light, the force and flux-density requirements are modest. However, finding a magnet to provide the low magnetic field while being large enough to be easily produced was a challenging task. A ceramic Indox V grade magnet was selected for its low energy product and linear demagnetization curve.

Knowing the pole face areas, the desired gap flux, and the demagnetization curve for Indox V, the magnet dimensioning became straightforward. H_m and B_m define the operating point of the magnet on the demagnetization curve. Normally, the magnet operating point is chosen such that the product $B_m \cdot H_m$ is greatest. This is where the magnet produces the most energy and hence, requires the least volume. In this case, however, it was desired to make the magnet somewhat larger than minimum to ease production problems. The operating point was set at B_m = 0.36 T and H_m = 1.6 x 10^4 amp·turns/meter. B_g has already been set at 0.14 T, the leakage factor σ_L was estimated at 1.1 and the reluctance factor σ_p at 1.25. The leakage factor is used to compensate for the fact that there are both leakage and fringing fields in the magnet circuit and reluctance factor, σ_p, to compensate for the drops in magneto-motive force (the magnetic equivalent to voltage) in the back iron. The final dimensions of the Indox V magnet are 14 mm long x 6.2 mm wide x 5.3 mm high. The magnet fits easily in the available space and is large enough to be easily manufactured.

The bias flux is modified by control coils to produce the differential forces that center the assembly. There are six coils per bearing set, one for each air gap. The basic coil design is simple - there are several issues that complicate matters, however. These are the packing factor, the leakage factor, and coil temperature use. The packing factor is only important when the final coil dimensions are determined. The factor, typically $\pi/4$, is used to account for the fact that not all of the area in a coil is occupied by copper.

Leakage, unlike packing, is a very serious issue in magnetic circuit design. The leakage factor is typically defined as the ratio of coil flux to gap flux:

$$\sigma_l = \frac{\sigma_{coil}}{\sigma_{gap}} \qquad (2)$$

where σ_{coil} is the magnetic flux produced by the coil, and σ_{gap} is the magnetic flux in the gap. A leakage factor for very efficient designs is about 1.05, but factors of 2 or more are not uncommon in large magnetic circuits. Initially, an estimate of 1.1 was used, and computer modelling using magnetic analysis software was performed for verification. The software operates by producing a finite element mesh over the user-entered magnetic structure and then solving for the magnetic potential on this mesh, subject to prescribed boundary conditions. The computer results supported initial estimates, giving leakage factors of 1.1 to 1.2. This is indicative of an efficient design with little flux loss.

Though the packing and leakage factors influence the coil design in an important way, the primary determinant of coil size is the limit on temperature rise. Though copper wire can carry significant currents under ideal conditions, the allowable current density is much smaller in practice. The limit in reality is power, more specifically the equilibrium temperature the wire will attain under steady current and whether the insulation and surrounding equipment can tolerate it. In other words, after the ampere-turns requirement is determined, the current density is set so that the steady state temperature of the coil is acceptable; this, in turn, sets the size of the coil. For this application, the final temperature rise should not be more than 50 C or so. Though a detailed thermodynamic analysis was not carried out, a value of $4 \cdot 10^6$ Amps/meter^2 was chosen for experience as a conservative estimate. The resulting power consumption for maximum force is 0.25 Watts for coil 1, and 0.15 Watts for coil 2.

The final step in the design procedure was selection of the magnetic materials to be used. The poles must be resistant to eddy current losses and so are designed to be made of silicon steel laminations. The shaft, however, must be able to carry the linear motor magnetic bearing flux. For this reason, Vanadium Permandur is the material of choice; it has very high saturation flux density.

Overall, the translator bearing design is simple and effective. The final design is shown in Figure 5. Though the size constraints are tight, the entire mechanism comfortably fits in available space. It appears that retrofit of this bearing into the current system is feasible and practical.

CONTROLLER CHARACTERISTICS

The attribute of the magnetic bearing configuration which has the largest influence on the controller design is the type of force employed. As discussed earlier, the choices are the primary

attraction force, or the secondary attraction force. The secondary attraction force is inherently stable and requires no external controller. The translator stage magnetic bearing employs the primary attraction force. This force is an unstable effect by its physical nature. A small change in the air-gap length (δG) produces a small change in force (δf_p) that tends to increase the change in the air gap at constant excitation. When this force is exerted on a body of mass m_b, application of Newton's law produces a differential equation for the position of the suspended body (x). If an increase in the position of the body is defined as a decrease in the air-gap length:

$$(\delta x) = -(\delta G) \tag{3}$$

the linearized differential equation about a nominal position (x_o) becomes the following:

$$m_b \frac{d^2(\delta x)}{dt^2} - c_g(\delta x) = c_i(\delta i) \tag{4}$$

Taking the Laplace transform and rearranging shows that an unstable plant results.

$$\frac{\delta x}{\delta i}(s) = \frac{c_i}{m_b s^2 - c_g} \tag{5}$$

The plant is characterized by a natural rate of growth (ω_u, typically called the "unstable frequency") which is calculated as follows:

$$\omega_u{}^2 = \frac{c_g}{m_b} = \frac{B_{go}{}^2 A_{go}}{\mu_o m_b G_o} \tag{6}$$

The unstable frequency of a given configuration is thus determined by the nominal (or bias) flux density.

The unstable plant that is represented by Equation (5) is characterized by a pair of real poles that are equally spaced about the imaginary axis ($s = +/- \omega_u$). The frequency response of the plant is characterized by both constant 180 degrees of phase lag over the entire spectrum and finite dc gain as shown in Figure 6. Stabilization of the closed loop response using classical lead-lag compensation of this plant is illustrated in Figure 7. Here the lead is introduced at the unstable frequncy (ω_u) and the lag occurs at $10\omega_u$. As shown, this results in approximately 45 degrees of phase margin. Since this technique is only successful above the unstable frequency, closed-loop stability requires a minimum bandwidth above ω_u.

POSITION SENSOR

The position sensors are probably the most vital element of the control system. In general, the controller can only be as accurate as its input information. Thus, for the high stiffness and accuracy

242

requirements of the magnetic bearing to be met, sensors of high resolution and accuracy are needed. Three types of non-contact position sensors were investigated to determine their suitability.

Photo-electric sensors are devices that use light to make distance measurements. Normally, they operate by measuring the intensity of light from a reflective target surface. As the target moves, the intensity of the reflected light changes, a change which is quasi-linear and can be measured. In static measurements, resolutions of one micron can be obtained. However, with surfaces of less than fine and uniform finish, or with a moving target, performance degrades rapidly. Another disadvantage to photo-electric systems is that two units (a transmitter and a receiver) are needed for each measurement. These two factors render these sensors inappropriate for the translator bearings.

Inductive sensors are very commonly used in metal sensing applications. They operate by using a high frequency oscillator to produce eddy currents in the target. As the target moves, the change in loss in the sensor circuit is measured. Resolutions of 0.025 mm are possible, and the sensors are readily available in small sizes. However, when measuring ferrous or moving targets, performance degrades rapidly. Since the sensors will be mounted in the moving translator, both of these conditions apply. This renders inductive sensors unsuitable for the bearings.

Capacitance sensors operate on a similar principle to that of inductive sensors, utilizing a high frequency alternating electric field (about 50 Khz). They do not require a metallic target and are free from the performance degradation problems of the inductive sensors. They are commercially available in a variety of very small packages and have resolutions to ten microns. Additionally, capacitive sensors offer excellent linearity and stability. For these reasons, capacitive sensors are the best choice for this magnetic bearing configuration.

The particular sensor chosen is model number ASP-20-PCR Pancake Radial Sensor from Mechanical Technology Instruments. It has an accuracy rating of +/-0.1% of range or 0.5 microns, and a resolution of 0.5 microns also. The specific model was selected such that the nominal air-gap length of 0.3 mm falls close to the middle of its linear range (0.5 mm). The overall dimensions of the sensor are 7.9 mm diameter and 2.5 mm thickness. Its extremely small size and high resolution make it an ideal candidate for this bearing system.

The proposed sensor locations are shown in Figure 8. The sensors will be epoxy mounted in depressions milled in the aluminum carriage and measure the distance between the carriage and the shaft (which is also the distance between the pole and the shaft). Small holes for the lead wires will also be needed, but these are minor modifications. Eight sensors will be used in total (two for each pole piece), providing double redundancy of information and hence more accurate support.

ELECTRONICS

The electronic functions required to close the control loops on the magnetic bearings are as follows:

(1) Position sensor interface
(2) Sensor signal processing
(3) Loop compensation
(4) Actuator signal processing
(5) Coil power driver

High reliability and low quiescent power dissipation dictate the goals of circuit simplicity and minimal part-count. These goals are best achieved with the use of analog circuitry. In addition, the lack of digital circuitry will eliminate the interference produced by high-speed switching and allow better signal-to-noise performance. The implementation of each of the above functions is described in the following paragraphs.

The position sensor interface provides the functions necessary to measure the variation in the capacitance of the sensor with displacement of the sensed object and to produce a linear voltage per displacement output. This is accomplished by exciting the sensor with a high-frequency ac current and measuring the ac voltage developed across the sensor. This voltage is then demodulated and filtered and corrected for its inverse proportionality to displacement. It is currently planned to purchase the unit which has been specially designed by the sensor manufacturer to interface to the selected position sensors.

The sensor signal processing must process the output of the eight sensors into the information required to control the five constrained degrees of freedom of the suspended translator head. The use of eight sensors results in the existence of redundant information. This redundancy will be accommodated by averaging signals with analogous information. The resultant signals will then be added to or subtracted from one another to produce translation and rotation information respectively. Implementing this function will require five operational amplifiers, one to produce the position signal for each of the five degrees of freedom.

The loop compensation circuitry multiplies the position signal for each control loop by the frequency dependent transfer function required to achieve the required stiffness and ensure loop stability. The specified integration is achieved with capacitive feedback around the operational amplifier resulting in approximately 120 db of open loop gain at dc. The remaining four poles and zeroes are produced by combinations of resistors and capacitors in either the input or feedback paths. Thus, again implementation will require only five op-amps, one per loop.

The actuator signal processing performs roughly the converse function to the sensor signal processing, i.e., it turns the five outputs from the control loop compensation stages into the six signals required to drive the actuator coils. Again addition and subtraction

of the signals is required and could be accomplished with six op-amps; however, the use of power op-amps in the coil power driver stages will allow implementation of both these functions in a single device per actuator.

The coil power drivers simply provide the voltage and current capability necessary to drive the actuator coils over their full force range. In order to keep the output-current requirement reasonable, it is planned to use +/-30 Volt power supplies for this stage. The use of separate power supplies for the power and signal stages also reduces the coupling of output power disturbances into the signal channels, thereby preventing parasitic feedback oscillations.

CONCLUSIONS

The overall technical objective of this program was to establish the technical feasibility of developing magnetic bearings for an optical disk buffer. The approach taken was to develop the specifications for the magnetic bearings and define the hardware configuration, controller characteristics, position sensors, and electronic functions required. Successful completion of these tasks is considered evidence of the technical feasibility of applying magnetic bearing technology to this device. The required electromagnetic hardware fits easily inside the available volume, and has reasonable power consumption. The position sensors are small and have excellent resolution and linearity. The controller requirements are modest as are the remaining electronic functions which need to be implemented. The extension of this design definition to the detailed design required for prototype development would appear to be an extremely straightforward effort.

BIBLIOGRAPHY

1. Downer, J.R., "Design of Large Angle Magnetic Suspensions," ScD Thesis, Massachusetts Institute of Technology, May 1986.

2. Levine, M.L., "A High Data Rate, High Capacity Optical Disk Buffer," 7th IEEE Symposium on Mass Storage Systems, Tucson, Arizona, November 4-7, 1985.

3. Roters, H., Electromagnetic Devices, New York: John Wiley & Sons, Inc., 1941.
4. Sabnis, A., "Analytical Techniques for Magnetic Bearings," PhD Thesis, University of California, Berkeley, June 1974.

5. Spin and Space Systems, Inc., Magnetic Suspension for Rotating Equipment, SBIR Phase I Final Report, Phoenix, Arizona, March 1980.

6. Studer, P.A., Magnetic Bearings for Instruments in the Space Environment, NASA Technical Memorandum 78048, Goddard Space Flight Center, Greenbelt, Maryland, 1978.

7. Watson, E.G., "Modal Analysis of Air Bearing Translator," RCA Internal Correspondence, January 1986.
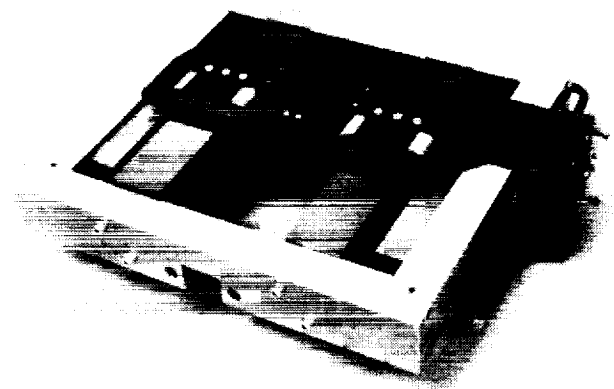
Figure 1. NASA/RCA translator assembly.

Permanent Magnets
and
Return Paths

Translator
Carriage

Support and
Air-Bearing
Shafts
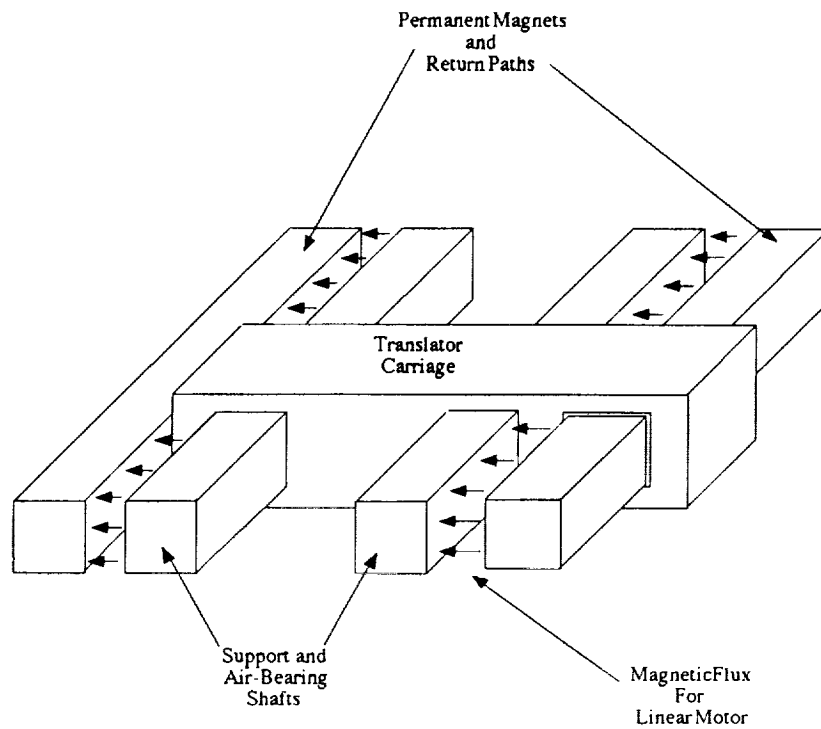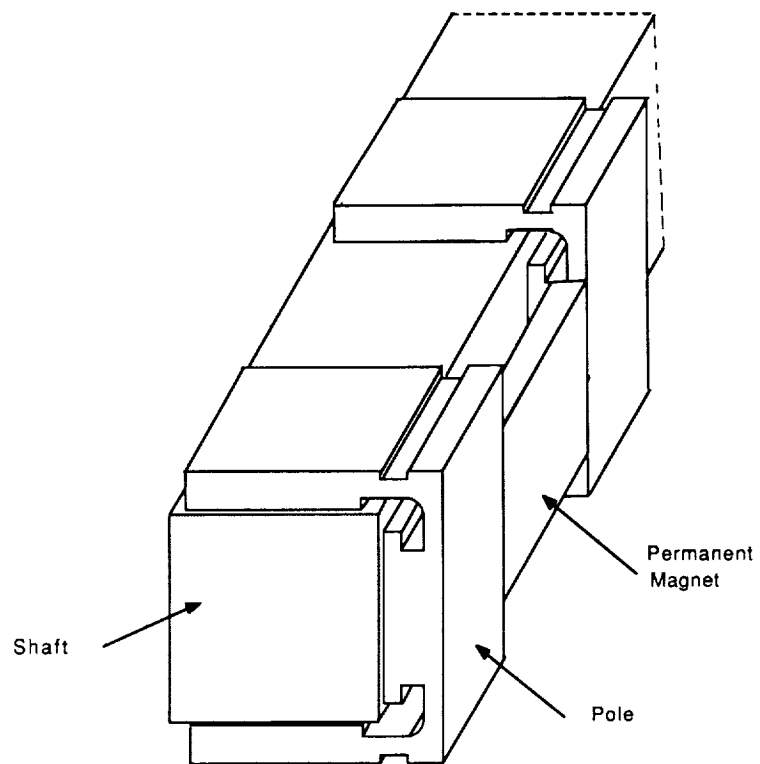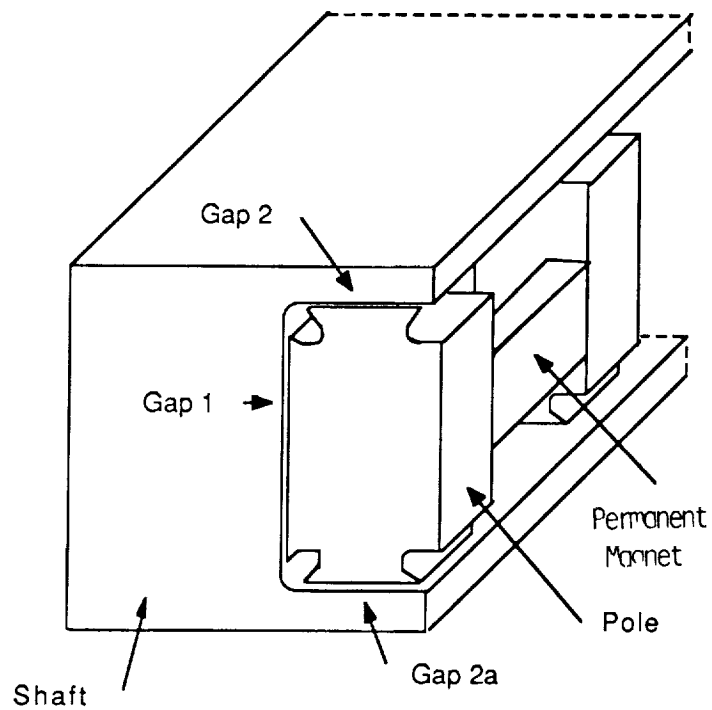
MagneticFlux
For
Linear Motor

Figure 2. Existing magnetic structure.

Figure 3. Preliminary bearing concept.

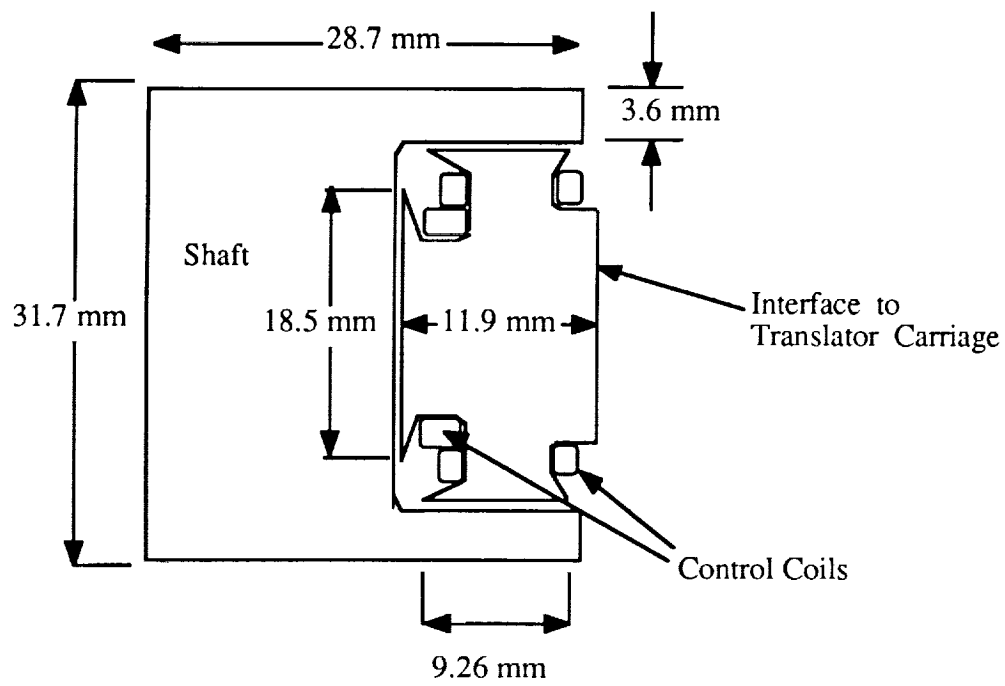**Figure 4. Candidate bearing concept.**
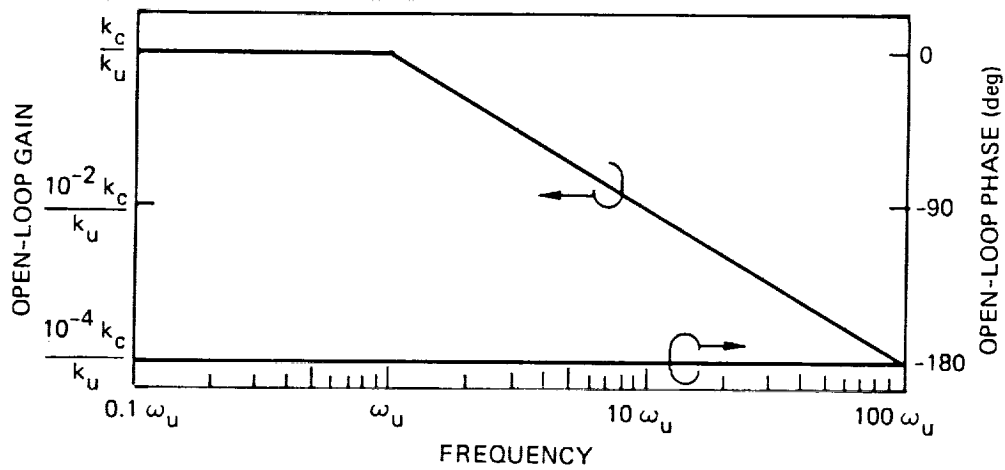
Figure 5. Translator bearing dimensions.
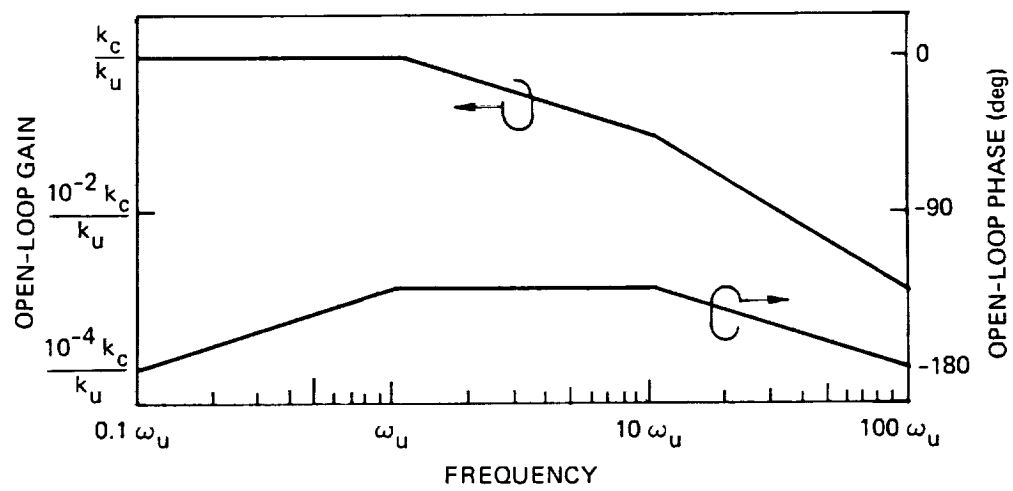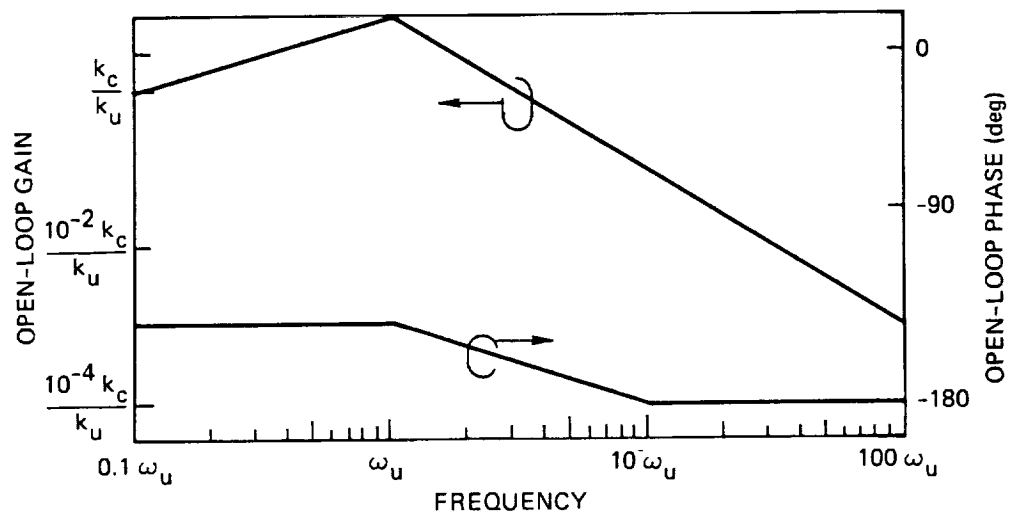

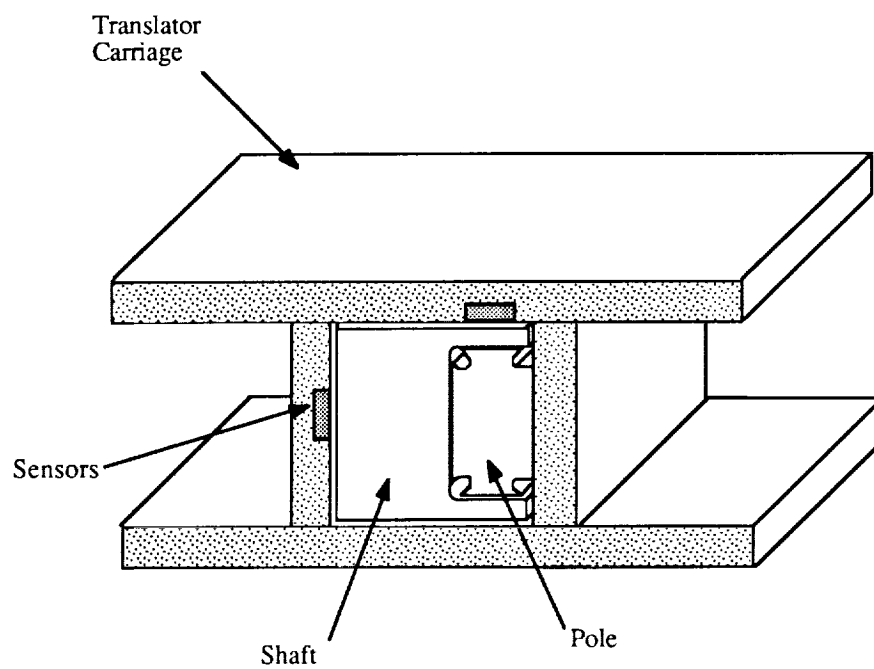Figure 6. Unstable-plant frequency response.

Figure 7. Lead-lag compensation of plant.

Figure 8. Position sensor locations.